

Cavitation inception

VIJAY H ARAKERI

Department of Mechanical Engineering, Indian Institute of Science,
Bangalore 560 012

MS received 19 June 1978; revised 26 September 1978

Abstract. In this paper, some general aspects of cavitation inception in flowing situations are considered. Special attention is paid to the problem of the scale effects commonly encountered by design engineers in extrapolating results from model tests to prototype situations. Past experimental and theoretical investigations relevant to the problem are reviewed. Recent advances in the field, particularly the influence of viscous effects in cavitation inception on smooth bodies, are discussed. Several useful scaling laws which are primarily based on empirical correlations or physical observations are suggested. A specific criterion which could be used to assess the importance of thermodynamic effects in cavitation inception is indicated.

Keywords. Cavitation; inception; viscous effects; scaling laws.

1. Introduction

One of the important differences between liquids and gases is that liquids can withstand tensile stresses whereas gases cannot. Theoretical predictions indicate that pure homogeneous liquids can withstand considerable tensile stresses, of the order of thousands of atmospheres. But if sufficiently strong tensile stresses are applied, the liquid ruptures to form cavities. In fact, even carefully treated liquid samples are known to withstand only a moderate tensile stress, of the order of hundreds of atmospheres. This discrepancy has led to the postulation of the presence of weak spots in the liquid samples, commonly known as 'nuclei'. The growth of these nuclei under the action of the tensile stress, resulting in visible cavities is termed 'cavitation inception'. It is obvious that if these cavities, once formed, are subjected to compressive stress, they should disappear. In general, cavitation is the study of the appearance, development and disappearance of cavities in a body of liquid.

Cavitation occurs commonly on ship propellers, in liquid-pumping devices, in flow control devices such as valves, gates and hydraulic spillways, and in other components which involve high-speed liquid flows. In addition, cavitation is an important part of the science of underwater ballistics and acoustics. An illustrative example of the nature and type of cavitation observed on a model ship propeller is shown in figure 1 (plate 1). As noted in a recent book by Knapp *et al* (1970), in almost all cases of practical importance, cavitation is an undesirable phenomenon resulting in the following adverse effects:

A list of symbols appears at the end of the paper.

- (i) reduction in efficiency,
- (ii) potential damage to the solid surfaces,
- (iii) presence of unsteady forces resulting sometimes in severe vibrations, and
- (iv) radiation of intense noise.

Among these, the effect most feared by design engineers is potential damage to the solid surfaces. An extreme example (Oosterveld 1977) was a ship propeller which came back for repairs with a large hole caused by cavitation in one of its blades in just seven days of open sea operations. To avoid such costly repair work, prototype devices have to be designed for cavitation-free operation.

The inception of cavitation, which determines the limit for cavitation-free operation, has been the subject of considerable experimental and theoretical research in the past few decades. Although much has been accomplished, many of the details of this phenomenon are still beyond our grasp. One is therefore forced to resort to model-testing to predict the conditions under which cavitation inception may take place in prototype devices. Unfortunately, the important factors governing cavitation inception have not been completely identified, and therefore extrapolation of results from model-testing to prototype conditions is fraught with uncertainties. As a result many unanticipated cavitation problems arise at the prototype stage although none existed during model tests.

Experience (see, for example, Holl & Wislicenus 1961) has shown that one of the important parameters useful in characterising cavitating flow has been the cavitation number defined as

$$\sigma = (p_{\infty} - p_v) / \frac{1}{2} \rho U^2, \quad (1)$$

where p_{∞} and U are reference static pressure and velocity respectively, ρ is the liquid density and p_v is the vapour pressure of the liquid at its bulk temperature. In water tunnel experiments, for example, p_{∞} and U refer to the tunnel static pressure and velocity respectively, measured sufficiently far away from the model. The value of σ at which cavitation inception takes place is designated σ_i . If σ were found to be the only important parameter in determining the conditions for cavitation inception, then we would expect the magnitude of σ_i to be the same for geometrically similar bodies. However, this is found to be contrary to experimental observations on various shaped bodies (Holl & Wislicenus 1961). The recurring features in this type of cavitation research are illustrated in figure 2 which is taken from the findings of Lindgren & Johnson (1966), a study sponsored by the International Towing Tank Conference. It is clear from this figure that σ_i can vary with the size of the body, tunnel velocity and possibly other parameters even for geometrically similar bodies. This dependence of σ_i on other physical parameters in determining the conditions for cavitation inception is commonly known as the 'scale effect'. The known dependence of σ_i on other physical parameters could then be termed as 'scaling law' or 'scaling rule'. One can arrive at a simple scaling rule by assuming that cavitation inception occurs as soon as pressure anywhere in the flow falls to the vapour pressure of the liquid. Since the minimum pressure, whether at the surface or in the interior of the flow, is the lowest available pressure, we get the scaling rule

$$\sigma_i = - C_p \min. \quad (2)$$

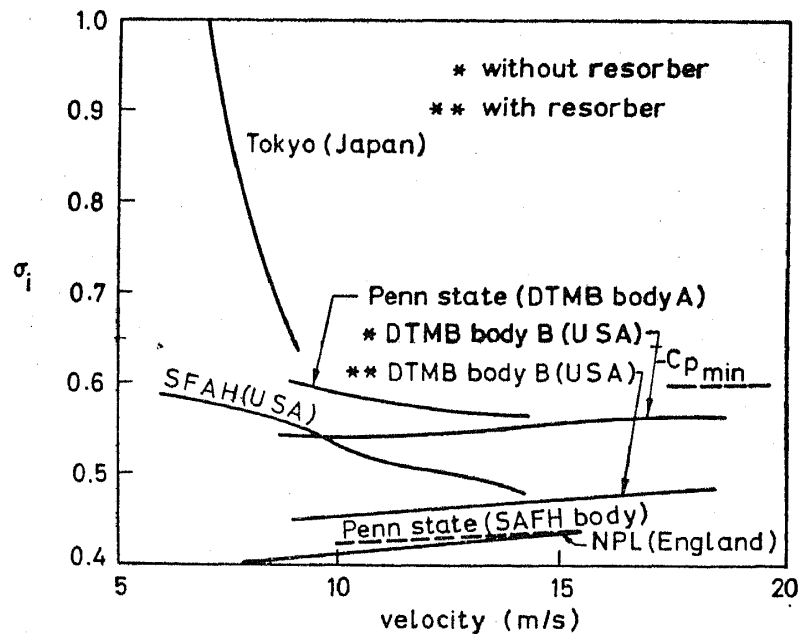


Figure 2. Comparative cavitation inception studies on geometrically similar axisymmetric bodies. Study sponsored by the International Towing Tank Conference (Lindgren & Johnson 1966).

Here, $C_{p \min}$ is the minimum value of the pressure coefficient C_p , which is defined as

$$C_p = (p - p_\infty) / \frac{1}{2} \rho U^2, \quad (3)$$

where p is the local static pressure. The scaling rule (2) is used so widely in practice that the deviations from it (see for example figure 2) are sometimes termed as scale effects. However, our definition of scale effects noted earlier is more general.

The problem of scale effects is at the heart of scaling difficulties commonly encountered by design engineers in extrapolating cavitation inception behaviour from one set of conditions to another, and this subject will be the focus of this paper. First, we cover the background, which includes some physical features of cavitation inception, results from early experimental investigations and theoretical models developed to analytically predict cavitation inception. Next, certain important effects which are likely to lead to the observed scale effects are identified and finally our conclusions are provided.

2. Background

2.1. Some physical features of cavitation inception

It has been noted earlier that 'nuclei' or weak spots explain the growth of cavities observed at cavitation inception even under moderate tensile stresses. One of the simplest models of a nucleus is the so-called 'free nucleus', which is a spherical bubble containing the vapour of the liquid and some permanent gas. To understand the role of nuclei in cavitation inception, it is helpful to consider the static stability

of such a free nucleus. The equilibrium condition for the pressures inside and outside a bubble of radius R is

$$p_i = p(R) + (2s/R), \quad p_i = p_g + p_v, \quad (4)$$

where s is the coefficient of surface tension, $p(R)$ is the pressure in the liquid adjacent to the bubble surface and p_i is the interior pressure in the bubble. This pressure is expressed as the sum of two partial pressures; one due to the gas contents p_g and the other due to the vapour contents p_v . If it is assumed that the mass of the gas inside the bubble does not change, that the gas inside contracts or expands isothermally and that it obeys the ideal gas law, then p_g is proportional to C/R^3 where C is a constant. Using this, the equilibrium condition becomes

$$p(R) = (C/R^3) - (2s/R) + p_v. \quad (5)$$

To consider the stability of the bubble to a small reduction in the pressure p , we evaluate the derivative $dR/dp(R)$ from (5) and find that at a critical condition it becomes infinite; this means that the bubble radius grows at an unbounded* rate and this certainly can be interpreted as cavitation inception. It is easy to show that the critical condition is given by

$$p_v - p_c = 4s/3R. \quad (6)$$

where p_c is the critical pressure. Figure 3 shows a plot of equation (6), and it is apparent that the critical pressure for cavitation inception is always less than p_v but will approach it for large values of R . In addition, if the liquid sample does not contain nuclei with radius greater than one micron (10^{-6} m), then we would not expect cavitation within the liquid unless the sample is subjected to *negative* pressures of the order of one bar. Therefore, the normal assumption that cavitation inception will take place as soon as pressure is reduced to the vapour pressure is strictly good only if the liquid sample contains nuclei of radii greater than about $100 \mu\text{m}$. This brings us to an important consideration of the nature and sources of cavitation nuclei in a liquid sample.

2.1a. Nature and sources of cavitation nuclei The weak spots in a liquid sample have been hypothesised (Flynn 1964) to be mainly of the form of gas bubbles, a non-wetting solid particle, a gas pocket trapped in a crack on the surface of a non-wetting solid particle or a gas pocket trapped in a crack on non-wetting solid surfaces coming into contact with the liquid sample. It is important to note that for the last two forms of nuclei the curvature of the gas-liquid interface should be such that the pressure in the liquid is greater than the pressure in the gas pocket. In this configuration the gas pocket will stay in an equilibrium whereas in the reverse situation the gas in the pocket will dissolve due to surface tension effects. These arguments are mainly due to Harvey *et al* (1947) and for this reason the types of nuclei with gas pockets are commonly referred to as 'Harvey nuclei'.

*This is physically unrealistic and one must consider complete dynamic equations once the critical condition has been reached.

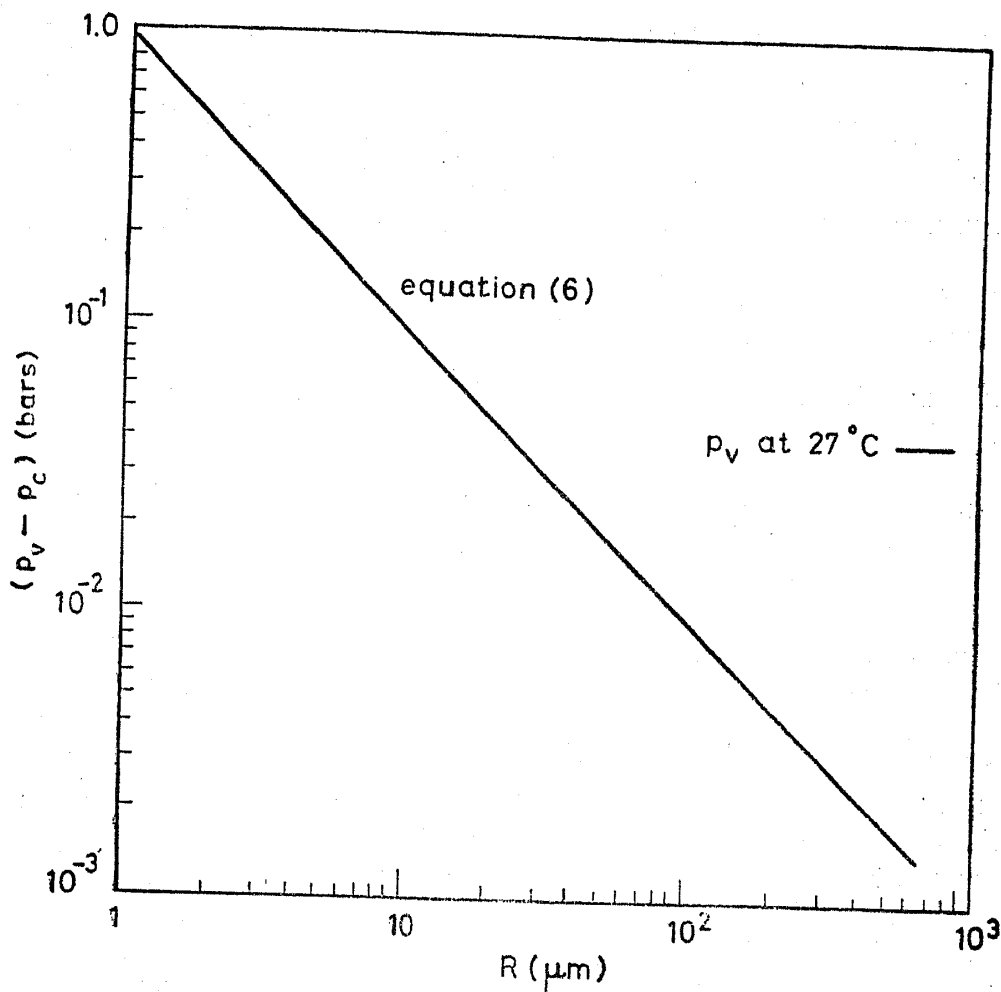


Figure 3. A plot of critical pressure versus bubble radius obtained from static stability considerations.

A necessary condition for the existence of a Harvey nucleus is that the solid be hydrophobic or non-wetting. In a freshly drawn water sample (for example from a tap) all types of nuclei will most likely exist; however, if the sample is left standing for a few hours under quiescent conditions then the larger air bubbles will rise to the surface, the smaller air bubbles will dissolve due to surface tension effects (Epstein & Plesset 1950) and the larger particles will settle down to the bottom. Therefore, only small particles with or without gas pockets stabilised by brownian motion will remain in the interior of the liquid sample as viable nuclei. From the above considerations we can infer that the size of nuclei in a quiescent liquid will be small; recent measurements of Keller (1972) indicate that they are of the order of only a few microns.

A different situation exists for a liquid recirculated in a test facility like a water tunnel. In this case, moderately large air bubbles or even solid particles can remain in the flowing liquid for significant periods of time. It has been found that gas bubbles are liberally generated in the region of high turbulent shear, like the downstream flow of the main circulating pump (Ripken & Killen 1962). These gas bubbles will appear in the test section unless special provision is made to put them back into the solution. Certain facilities do incorporate a special feature in the water tunnel circuits known as 'resorber' to effect the dissolution of air bubbles. This is accomplished by subjecting the flowing liquid with air bubbles to high pressures for significant

periods of time in the resorber. Thus, the nuclei content of the liquid flowing in water tunnel facilities is largely dependent on whether they are provided with resorbers or not, other conditions being the same. Certainly the observed scale effects in figure 2 can be explained partly by the fact that some of the test facilities were equipped with resorbers whereas others were not. Therefore, it is clear that nuclei of various sizes can exist and the next question to consider is how they grow to visible cavities.

2.1b. *Growth potential of a nucleus* Photographic observations of cavitation inception show that basically two types of bubble growth exist; namely,

- (i) explosive growth with a time scale of the order of milliseconds, and
- (ii) slow growth with a time scale of the order of seconds.

The first type, also considered in our static stability analysis, is commonly referred to as 'vaporous cavitation' and the second type as 'gaseous cavitation'. Vaporous cavitation is possible only if the nucleus experiences pressures equal to or below the vapour pressure of the liquid. Gaseous cavitation is possible at any pressure but the gas content in the liquid should be supersaturated to partial pressure of gas inside the cavity and the nucleus should be subjected to this condition for extended periods of time. It must be pointed out that the above distinction is simply a description of the observed physical effects and we do not claim to know the contents of the cavity for the two different types of cavitation. However, it is most likely that for the second type of cavitation significant amounts of permanent gas are present inside the cavity because of gaseous diffusion. It is commonly recognised that vaporous cavitation is dangerous and gaseous cavitation can play a confusing role in the identification process (Holl 1969). Thus, the growth of a nucleus is primarily influenced by the nature of the pressure field it experiences.

2.2. *Results from some experimental investigations*

The material presented in §§ 2.2 and 2.3 has been covered in some detail by Holl (1969). However, since Holl's review article was written, significant new advances (to be covered in §§ 3 and 4) in the field have been made and in the light of these, new interpretations of the earlier experimental and theoretical investigations are needed. Therefore, it was felt worthwhile to briefly cover some of the earlier investigations as a prelude to the subject matter covered in §§ 3 and 4.

Experimental studies on cavitation inception in the past consisted of two categories; those which can be termed as cavitation scaling experiments and others which can be called cavitation mechanism experiments.

2.2a. *Cavitation scaling experiments* In these, many different shaped bodies have been used for inception observations to determine the important dimensionless parameters such as Reynolds number and Weber number, which would assist in developing proper scaling laws. The studies are normally conducted in a water tunnel which provides control of the test section static pressure independent of the velocity. Inception observations are generally made by holding the velocity fixed and lowering the tunnel static pressure slowly until signs of cavitation appear. Another technique used is to first establish a cavity and then raise the static pressure

slowly until signs of cavitation disappear. The point of disappearance is termed 'desinent' cavitation by Holl (1960a). The criterion most often used for inception or desinence is based on visual observations of a macroscopic cavity in the regions of low pressure. This method does introduce some arbitrariness in the definition of cavitation inception, and improved methods based on acoustic and optical techniques are being used and pursued. Some typical results of inception measurements by Parkin & Holl (1954), Parkin (1952) and Kermeen & Parkin (1957) are shown in figures 4, 5, and 6 respectively. The results in figure 4 are for two sets of geometrically similar axisymmetric bodies with different nose shapes. Inception characteristics of geometrically similar two-dimensional hydrofoils are shown in figure 5 and finally results for a bluff body shape are presented in figure 6. It should be noted that for a bluff body σ_i is primarily a function of Reynolds number whereas this is not the case for the axisymmetric bodies or the two-dimensional hydrofoils. The latter show a size dependence for a fixed Reynolds number. In general, studies of the type shown in figures 4, 5 and 6 have indicated certain general trends like the usefulness of the Reynolds number as a correlating parameter; however, they have not identified all the pertinent parameters of importance in cavitation inception scaling.

2.2b. *Cavitation mechanism experiments* These are of a more fundamental nature and are concerned with the bubble dynamics aspects of cavitation inception. As

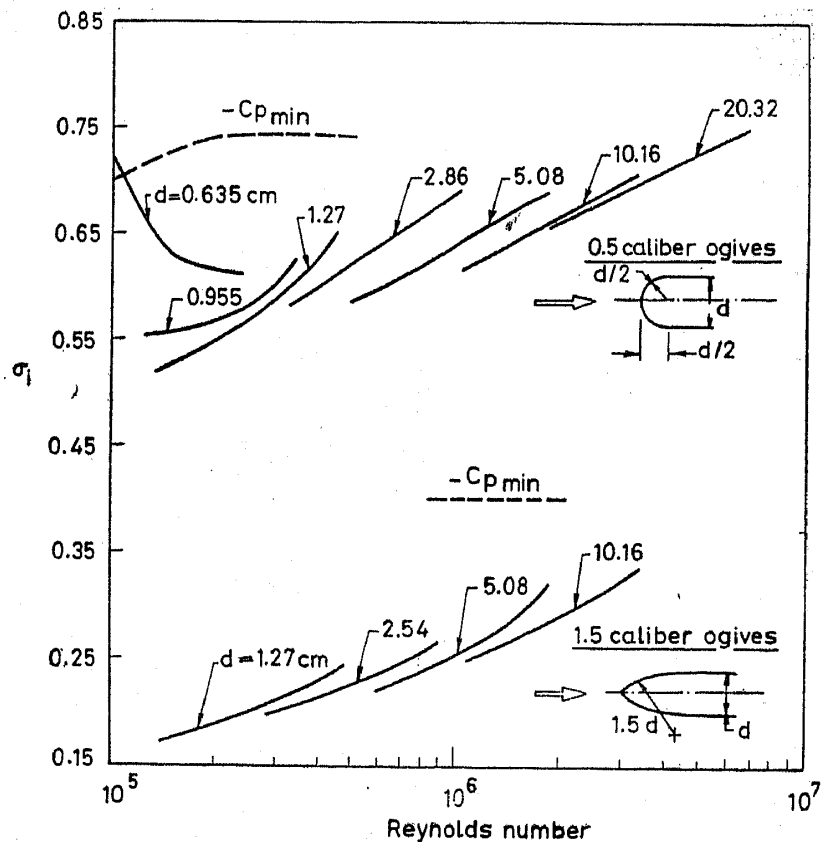


Figure 4. Cavitation inception number versus Reynolds number based on maximum diameter for various sized axisymmetric bodies with two different nose shapes (Parkin & Holl 1954).

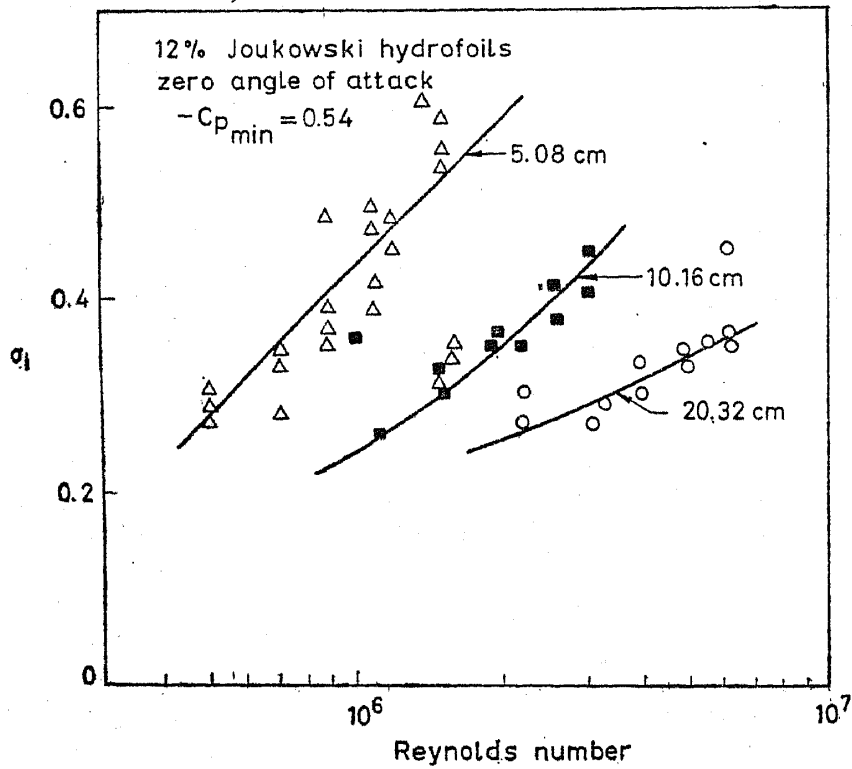


Figure 5. Cavitation inception characteristics of three different sized 12% Joukowski hydrofoils at zero angle of attack. The Reynolds number is based on the chord length (Parkin 1952).

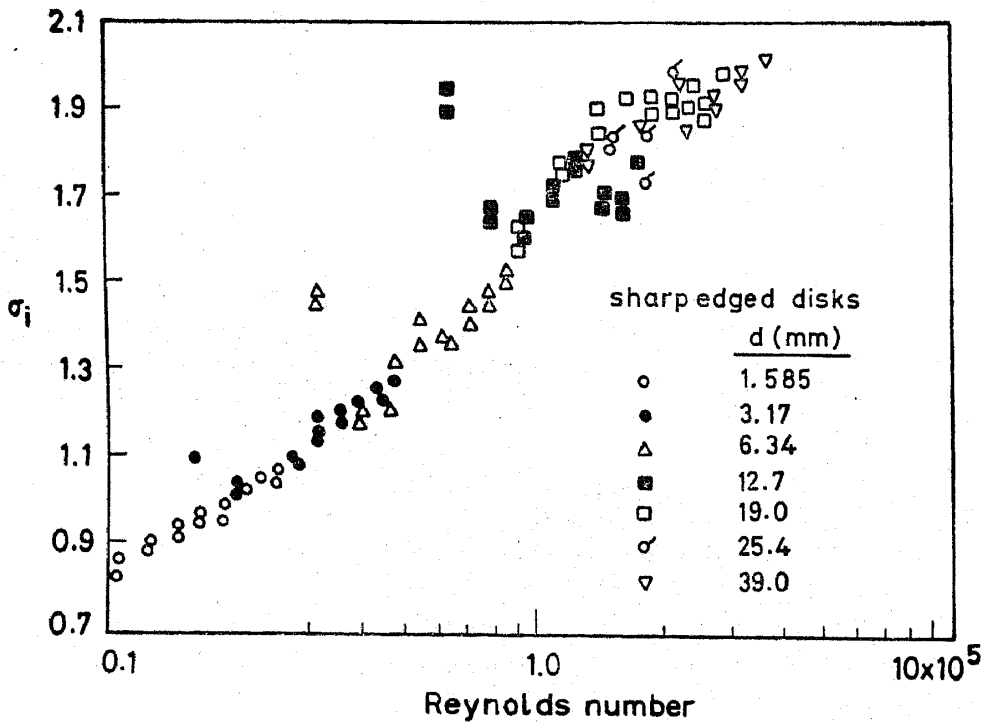


Figure 6. Cavitation inception number versus Reynolds number for various sized sharp edged disks (Kermeen & Parkin 1957).

early as 1948, Knapp and Hollander obtained photographs of bubble growth patterns at cavitation inception on a streamlined body with framing rates of 20,000 frames per second. The observations revealed that the cavitation bubbles originating within the free stream travelled at a velocity approximately equal to the free stream liquid velocity. Thus, the 'travelling bubble' type of cavitation inception was apparently not influenced by the boundary layer effects; but, on a different shaped body, Parkin & Kermeen (1953) observed cavitation bubble growth taking place within the boundary layer region of the flow. They photographed complex bubble growth patterns where extremely small bubbles (0.05 mm) were observed to grow at a fixed point on the surface until they reached a certain height when they were swept downstream to form into macroscopic-sized cavities. The bubble velocities were found to be significantly lower than the free stream liquid velocity and under certain circumstances the bubbles were observed to move in the reverse direction to the main flow. Thus, this 'surface' or 'attached' type of cavitation was significantly influenced by the boundary layer or viscous effects. In a later study, Kermeen & Parkin (1957) photographed cavitation bubble growth taking place in the flow downstream of a disk. They observed certain rotational patterns of a pair of cavitation bubbles strongly indicating that inception was taking place within the vortices shed downstream of the disk. This observation was supported by flow visualisation studies. Thus, it is expected that this 'vortex' type of cavitation inception will be influenced by viscous effects and as noted earlier the σ_i values for the disk show predominantly a Reynolds number dependence (figure 6).

These studies bring out three different types of cavitation at inception, namely: travelling bubble, surface or attached and vortex. Photographs of the three types are shown in figure 7 (plate 2) (items 1, 3, 7 and 8), figure 7 (plate 2) (items 2, 4, 5, 6 and 9) and figure 1 (plate 1) respectively. The studies, in addition, do give some insight into the possible sources of the observed scale effects, and for this reason, have been the basis for the many theoretical models developed to predict the observed scale effects.

2.3. Theoretical models

In general, the theoretical prediction of cavitation inception is based on calculations of the growth of a spherical bubble from an initial radius R_0 to a prescribed final radius. The behaviour of a single spherical bubble is assumed to characterise the problem. The bubble growth is determined by the solution of the Rayleigh-Plesset equation (Holl 1969). The pressure distribution used in the calculation is that existing under non-cavitating conditions.

One of the first rigorous attempts to model the process of cavitation inception was made by Parkin (1952). It was supposed that cavitation was initiated from small nuclei which contain air or water vapour, or both, stabilised on small solid particles in the liquid. Based on stability arguments and experimental observations these nuclei were taken to be spherical bubbles of radius 2×10^{-4} mm. The bubble was assumed to travel along the model surface at the local liquid velocity and cavitation inception was said to occur when the bubble radius reached a value of 1 mm. Calculations carried out using the model for the hemispherically-nosed bodies (0.5 caliber ogive) showed poor agreement with the observed values. Parkin attributed the lack of agreement between theory and experiment to the neglect of the boundary layer

effects. It was only after Parkin & Kermeen's (1953) experimental observations became known that Oshima (1961) and Van der Walle (1962) incorporated boundary layer effects in developing theoretical models for cavitation inception. Oshima considered dynamic similar growth of cavitation bubbles specified by the Rayleigh-Plesset equation and the key assumption he made was that cavitation occurs when the diameter of a growing bubble reaches a value equal to that of the local boundary layer displacement thickness. This assumption, which is a direct consequence of Parkin and Kermeen's experimental observations, introduced a Reynolds number and size dependence on σ_i which compared well with the experimental observations. Van der Walle (1962), on the contrary, considered the growth dynamics of a cavitation bubble to be influenced by boundary layer effects. He studied the possibility of gaseous and vaporous growth of both the free stream and surface nuclei and a hypothesised process of a surface nucleus being generated from a crevice. He concluded that the surface nuclei generation, their detachment and subsequent behaviour will be influenced by a balance of local pressure gradient forces, inertial drag forces, viscous drag forces and surface adhesion forces. In particular, he pointed out the possibility of the stabilisation of nuclei in the boundary layer as a result of adverse pressure gradient forces. Thus, for different bodies with different pressure gradients, Van der Walle obtained various inception relations and, accordingly, scaling factors. Comparison of his theoretical calculations of σ_i on a hemispherically-nosed body showed only a qualitative agreement with the experimental results. More recently, Holl & Kornhauser (1970) have formulated a theoretical model which combines the basic ideas of Parkin (1952) and some of the concepts introduced by Van der Walle (1962). They conducted extensive studies on the effects of initial conditions, stream versus surface nuclei and thermodynamic effects on cavitation inception. In general, they found good qualitative agreement with experiments; however, they were unable to observe the strong thermodynamic effects predicted from their theoretical calculations.

The theoretical models considered so far make certain assumptions concerning the nature and size of nuclei available for cavitation inception. It is easily shown (Holl 1969) that if the initial size of the nuclei is assumed to be sufficiently large, then, the scaling rule $\sigma_i = -C_{p \min}$ should become valid in the absence of boundary layer effects. However, this is found to be contrary to experimental observations (Schiebe 1969) even in tunnel facilities where a copious supply of large free stream air bubbles is known to exist. In this regard, Johnson & Hsieh (1966) have made an important contribution in explaining the discrepancy just noted. They analytically showed that due to pressure gradient effects ahead of a body there is a 'screening' process which tends to deflect the easily cavitable larger bubbles away from the minimum pressure point. This leaves only the smaller bubbles as potential cavitation nuclei even though the larger ones are present in the flow. The screening effect leads to speed and size dependence of σ_i which is consistent with our observations.

We might note here that the predicted σ_i based on all the preceding theoretical models with the exception of Johnson & Hsieh are compared with experimental observations (figure 4) of σ_i on a hemispherically-nosed body (0.5 caliber ogive). Recently, it has been found by Arakeri & Acosta (1973) that the cavitation inception on a hemispherically-nosed body is strongly influenced by the existence of a laminar separated region even up to a body Reynolds number of one million. None of the theoretical models considers this possibility at these or even lower Reynolds numbers.

In fact, assumptions like turbulent transition near the minimum pressure point (Holl & Kornhauser 1970) or the neutral stability point (Oshima 1961) which precludes the possibility of laminar separation are made. In view of this, the good agreement found by Oshima between his calculations and experimental observations should be considered fortuitous. Nevertheless, the theoretical models developed, with the exception of Oshima's, are general in nature and hence should prove to be useful in predicting σ_c under circumstances where the assumptions made by various investigators in developing individual theoretical models are likely to be valid. In fact, Plesset (1949) found excellent agreement between the calculated and observed growth and collapse phases of cavitation bubbles which were travelling outside the boundary layer region of the flow.

3. Influence of nuclei content on cavitation inception

Until recently, the problem of nuclei was treated either qualitatively or was based on assumptions; this is apparent from the theoretical models considered in the previous section. However, several techniques are now available (Morgan 1972) which could be used to directly measure the size and number distribution of the nuclei content of a

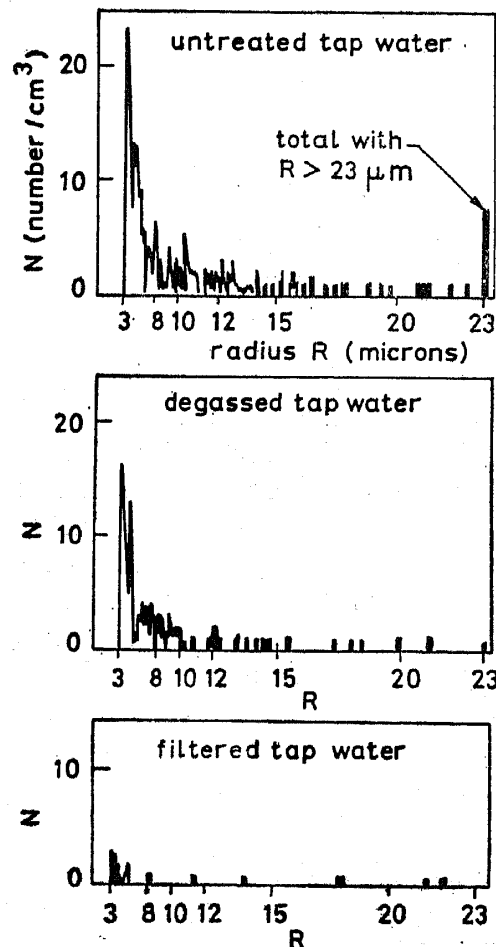


Figure 8. Measured nuclei size distribution for untreated and treated tap water by the laser light scattering technique (Keller 1974).

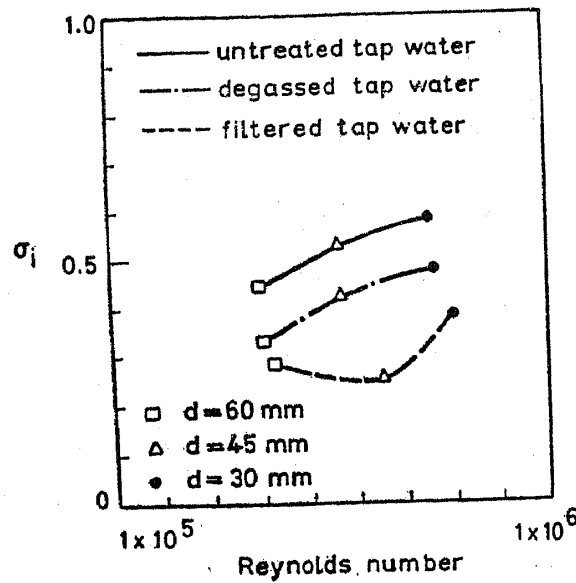


Figure 9. Cavitation inception characteristics of hemispherically nosed bodies as influenced by water quality (see figure 8 for corresponding nuclei size distribution); after Keller 1974.

liquid sample. Two techniques, among the many developed, namely (i) laser light scattering techniques (Keller 1972) and (ii) holographic methods (Peterson 1972), show promise for practical applications. Some measurements of nuclei size distribution in the free stream, made by laser light scattering techniques are shown in figure 8. However, it must be noted that from the work of Johnson & Hsieh (1966) we may expect the nuclei size distribution critical for cavitation inception to be different from the nuclei size distribution measured upstream of the body, due to the screening effect. In fact, several authors (Schiebe 1969; Peterson 1972; Gates 1977) have used the measured nuclei size distribution to infer the number of cavitation events with the inclusion of screening effect. In general, they have found good qualitative agreement with the measured number of cavitation events. The cavitation inception considered and observed was the travelling bubble type and from the measurement of Keller (1974) shown in figure 9 it is apparent that this type of cavitation inception is strongly influenced by the nuclei content of the liquid. However, on a body similar to the one tested by Keller, Gates (1977) found very little influence due to change in the nuclei size distribution on σ_i for the attached type of cavitation inception. The discrepancy may be due to the different types of cavitation observed at inception or due to the fact that Keller was able to drastically alter the nuclei content of his liquid sample whereas Gates was not. In any case, it would be very useful to measure nuclei size distribution under various testing conditions as well as under prototype situations. Once this is available it may be possible to estimate the critical pressure p_c for each liquid sample and then work with a modified cavitation number based on p_c rather than p_v for scaling purposes.

4. Viscous effects on cavitation inception

4.1 Inception on smooth bodies

By smooth bodies, we mean bodies whose boundaries have a continuously turning

tangent plane and which otherwise are 'hydraulically' smooth. Progress made in understanding the inception characteristics of such bodies is primarily due to the development of flow visualisation techniques, namely schlieren (Arakeri 1973; Gates 1977) and holographic interferometry (Van der Muelen 1976), in observing details of the boundary layer flows in water at high Reynolds numbers. These two optical techniques have proved to be considerably more sensitive than the ones used normally (dye injection, oil film, hydrogen bubble etc). In addition, these optical methods offer an advantage in that the viscous flow past a body and its cavitation inception characteristic can be observed simultaneously. A photographic illustration of such observations from the work of Arakeri & Acosta (1973) is shown in figure 10 (plate 3). These observations have since been repeated by Van der Muelen (1976) and Gates (1977). In figure 10a (plate 3) the macroscopic bubbles at cavitation inception appear in the reattachment zone of a laminar separated region. Subsequent reduction in pressure results in the separated region being filled with macroscopic bubbles (figure 10b) and finally with additional reduction in pressure an attached cavity is formed with a glossy smooth surface at the leading edge (figure 10c). Similar observations (Arakeri & Acosta 1974) in the absence of laminar separation have shown that cavitation in limited form appears in the turbulent transition region of the flow.

Therefore, turbulent transition location, whether it be on the free shear layer or within an attached boundary layer, is a critical zone for cavitation inception. One of the reasons for the above observation is the existence of strong pressure fluctuations in the critical zone, measured by Arakeri (1974) and Huang & Hannan (1975). The peak magnitude in the reattachment zone was of the order of 30% of the dynamic head. In addition, the wall pressure fluctuations in the transition or reattachment location were significantly greater than those existing in the developed turbulent region downstream. The theoretical models discussed in the previous section do not account for these pressure fluctuations; nor do they consider the likely role of the existence of laminar separation and other real fluid features on the dynamic aspects of bubble growth. In addition, future progress in developing theoretical models appears difficult since we still do not fully understand the pressure field experienced by a nucleus as it is brought into the region of separation followed by reattachment or turbulent transition within the attached boundary layer.

However, the recent observations just noted, coupled with the measured value of σ_i , suggest the following useful correlations to predict cavitation inception.

$$\sigma_i = -C_{ps} \quad \text{for flows with laminar separation and attached type of cavitation at inception (figure 10c, plate 3),} \quad (7)$$

$$\sigma_i = -C_{ps} + C_p \quad \text{for flows with laminar separation and bubble type of cavitation at inception (figure 10a, plate 3),} \quad (8)$$

$$\sigma_i = -C_{ptr} \quad \text{for flows without separation and attached type of cavitation at inception.} \quad (9)$$

C_{ps} is the pressure coefficient at the location of laminar separation, and C_{ptr} is the pressure coefficient at the location of turbulent transition. C_{ps} may be estimated by Thwaites' (Curle & Skan 1957) method and C_{ptr} by Smith's e^9 method (Jaffe *et al* 1970). C_p is to account for the measured strong pressure fluctuations in the region of

reattachment. The noted correlations explain many features of cavitation inception on smooth bodies (Arakeri & Acosta 1973; Huang & Peterson 1976). Using the correlation $\sigma_i = -C_{ptr}$, the observed dependence of σ_i on Reynolds number for the 1.5 cal ogive (figure 4) can be traced to the movement of turbulent transition location upstream on the model with increase in Reynolds number. The observed size dependence (figures 4 and 5) of σ_i is most probably buried in the fluctuating component of the pressure field since we do not expect a size dependence on the terms C_{ps} and C_{ptr} .

Another implication of the proposed correlations is that if laminar separation is eliminated and at the same time the location of turbulent transition is moved deliberately—let us say by tripping in the stagnation regions* of the flow—attached or surface type of cavitation should not be observed even if the σ value in the test section is lowered to the minimum possible magnitude. This was attempted (Arakeri & Acosta 1976) on a hemispherically-nosed body and the results were quite dramatic as shown in figure 11. At the critical Reynolds number it was impossible to sustain an attached cavity at σ as low as 0.25; it may be noted that without the trip, attached cavitation is observed at σ of about 0.7. Schlieren observations of the boundary layer flow showed that as the critical Reynolds number was approached the existing laminar separation was suppressed, and that most probably the location of turbulent transition had shifted close to the trip itself.

4.2 Influence of disturbances

From considerations in the previous section we would expect that any modification of the viscous flow past a body due to the presence of disturbances will have an indirect

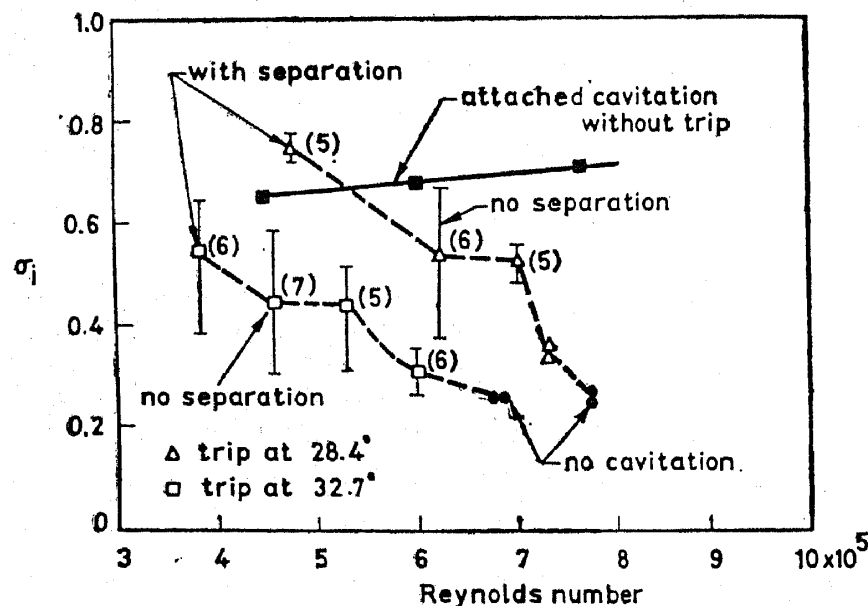


Figure 11. Cavitation inception number versus Reynolds number for 46 mm hemispherically nosed body with 0.127 mm boundary layer trip. Numbers in parentheses are the number of data points, the bars showing the range. The dominant type of cavitation for every test point was an attached cavity (Arakeri & Acosta 1976).

*Then C_{ptr} will be positive and thus predicted σ_i will be negative, which will imply a reference pressure below vapour pressure.

effect on cavitation inception. The disturbances can be 'natural' to the flow or can be deliberately introduced, in which case it will be termed as 'stimulated'.

4.2a Natural disturbances It is well-known that the presence of surface roughness, whether in the form of isolated roughness elements or distributed roughness, can influence the location of turbulent transition. Several techniques, mostly empirical in nature, have been proposed to predict the influence quantitatively (Tani 1961). One could use this information to predict the location of turbulent transition and then apply the scaling law $\sigma_i = -C_{prt}$ to predict the conditions for cavitation inception in the presence of surface roughness. However, it is expected that this procedure of predicting σ_i will not be accurate since the scaling law does not take into account the likely alteration in the pressure field due to the presence of surface roughness. No significant attempts have been made to measure the altered pressure fields; on the other hand, detailed investigations have been carried out to measure the σ_i values directly for isolated irregularities of various shapes placed on a flat plate. The data correlate well with the expression (Bohn 1972)

$$\sigma_{if} = C(h/\delta)^m (U_e \delta/\nu)^n; \quad 0 < h/\delta \leq 5, \quad (10)$$

where σ_{if} is the cavitation inception number in the presence of roughness on a flat plate, h is the height of the roughness element, δ is the local boundary layer thickness, U_e is the velocity at the edge of the boundary layer and ν is the kinematic viscosity. The values of the constants C , m and n suggested by Bohn (1972) for several types of irregularities are given in figure 12. Similar investigations by Arndt & Ippen (1968) for distributed roughness have shown that the data correlate well with the relationship

$$\sigma_{if} = 16 C_f, \quad (11)$$

where C_f is the coefficient of friction. The form of equation (11) may be explained by the fact that the source of cavitation in a turbulent boundary layer on a flat plate is

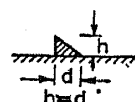
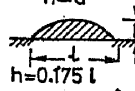
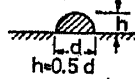
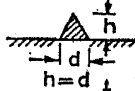
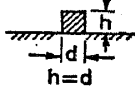
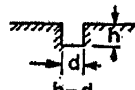
irregularity	flow dimensions	m	n	C	
triangles	two	0.361	0.196	0.152	
circular arcs	two	0.344	0.267	0.041	
hemispheres	three	0.439	0.298	0.0108	
cones	three	0.632	0.451	0.00328	
cylinders	three	0.737	0.550	0.00117	
slots	two	0.041	0.510	0.000314	

Figure 12. Magnitude of the constants C , m and n in equation (10) for various shaped isolated surface irregularities (Bohn 1972).

the existence of unsteady pressures which in a non-dimensional form are proportional to C_f (Blake 1970). The knowledge of σ_{if} for a flat plate can be used to predict the cavitation inception number, σ_{iR} for an isolated roughness element or for distributed roughness on an arbitrary body using the expression proposed by Holl (1960b),

$$\sigma_{iR} = -C_p + \sigma_{if} (1 - C_p), \quad (12)$$

where C_p is the pressure coefficient at the location of the roughness element on the parent body. For uniformly distributed roughness, the most logical choice for C_p in (12) would be the minimum pressure coefficient, $C_{p \min}$.

Besides surface roughness, the location of turbulent transition is also known to be influenced by body vibrations and the level of free-stream turbulence. In the presence of these disturbances, it may be sufficient to estimate the altered location of turbulent transition and then use the scaling law to predict the conditions for cavitation inception. A systematic study of the effect of body vibration on the location of turbulent transition is lacking. However, the role of free-stream turbulence has been the subject of past research, and semi-empirical correlations have been proposed by, among others, Vandriest & Blummer (1968) to predict the effect quantitatively. However, Gates (1977) has recently found that the effect predicted by the correlations is not always observed. For example, laminar separation on a hemispherically-nosed body could not be eliminated by increasing the free-stream turbulence level from a normal value of 0.04% to 3.75% at a body Reynolds number of 2.5×10^5 whereas the correlation due to Van Driest & Blummer predicts that laminar separation should have been eliminated with a free-stream turbulence level of about 1% at that Reynolds number. On a different axisymmetric body, the predicted effect was observed. Therefore, it appears that the level of free stream turbulence can affect the transition process only on selected body shapes for a fixed value of body Reynolds number. In this context, the findings of Gates (1977) should be kept in mind while comparing results of cavitation inception studies conducted in various flow facilities possessing different levels of free-stream turbulence.

During his studies, Gates also found another type of disturbance which is unique to water tunnel facilities. He observed that existing laminar separation could be eliminated by the presence of a significant number of macroscopic air bubbles in the free stream. This change in the viscous flow characteristics resulted in the travelling bubble type of cavitation at inception in place of the normally occurring attached type of cavitation. Again it should be noted here that several facilities not equipped with a resorber can have a copious supply of macroscopic air bubbles in the flow. The supply of these can not only alter the nuclei content of the liquid sample but can also influence the viscous flow characteristics of the body as just noted.

4.2b Stimulated disturbances It may seem attractive to use boundary layer tripping in the stagnation regions of the flow to simulate high Reynolds numbers as commonly done for aero- or hydrodynamic drag measurements. However, in the light of the findings by Arakeri & Acosta (1976), this can be a dangerous practice for cavitation inception studies. As shown in figure 11, on a tripped hemispherically-nosed body the σ_i value was found to decrease with increase in the Reynolds number contrary to the normal experimental observations of increase in the σ_i value with increase in the Reynolds number. This behaviour is attributed to drastic alteration in the location

of turbulent transition by tripping. Therefore, if tripping is to be used for high Reynolds number simulation, then the turbulent transition location should be carefully matched to the expected location at the higher prototype Reynolds numbers. In practice, this would be exceedingly difficult to achieve primarily due to the fact that the trip itself should not be the source of premature cavitation. Thus, even though tripping does not appear to be a promising technique to simulate high Reynolds numbers it does indicate a possible technique of delaying the onset of cavitation.

Somewhat similar effects have also been observed by the addition of dilute polymer solutions to the tunnel water. Essentially identical effects have been found either by injecting the dilute polymer solution at the nose of the body or by directly mixing the polymer solution to the tunnel water. When the effect was initially discovered by Ellis *et al* (1970), the reasons for the delay in the onset of cavitation were not apparent. Only recently, Van der Muelen (1976) and Gates (1977), using the optical techniques of flow visualisation, have shown that the effect of the polymer solution is to eliminate the existing laminar separation thereby effecting cavitation inception. Van der Muelen observed that the presence of polymer solution can decrease the critical Reynolds number for a smooth hemispherically-nosed body by an order of magnitude.

4.3 Turbulence effects

In contrast to laminar flow, fluctuating pressures can be a significant component of the total pressure field in turbulent flows. Then, in general, the incipient cavitation index could be written in the form (Arndt 1974)

$$\sigma_i = -\bar{C}_{p \min} + K_1(\overline{p'^2}/\frac{1}{2}\rho U^2), \quad (13)$$

where $-\bar{C}_{p \min}$ is the pressure coefficient based on average minimum static pressure. The factor K_1 takes into account the statistics of the pressure field. In particular, this factor is needed since it is not known whether the root mean square (rms) or the peak value of the pressure fluctuations is important for cavitation inception. We might note here that the form of equation (13) suggests that it is suitable for predicting σ_i for travelling bubble type of cavitation inception. However, direct use of this equation is difficult since very few measurements of rms pressure fluctuations in turbulent flows exist. In particular, measurements within the flow pose great instrumentation difficulties (Fuchs 1972), and indications are that the peak energy in turbulent pressure fluctuations is found in the centre of the mixing layer, whether it be a free shear flow or a wall-bounded flow (Arndt 1974). Due to lack of sufficient information, the prediction of cavitation in turbulent flows is based on empirical correlations. With the available data on cavitation inception and pressure fluctuations in turbulent flows, Arndt (1974) has proposed a scaling law of the form,

$$\sigma_i = -\bar{C}_{p \min} + 16 C_f, \quad (14)$$

where $C_f = -\tau_0/\frac{1}{2}\rho U_e^2$ for boundary layers, (15)

$$= -\overline{u'_1 u'_2}/U_0^2 \text{ for jets and wakes;} \quad (16)$$

τ_0 is the wall shear stress, $\overline{u'_1 u'_2}$ is proportional to the turbulent Reynolds stress, U_e is the velocity at the edge of the boundary layer and U_0 is the mean velocity. The correlation (14) is based on cavitation inception observation in both fully developed and transitional turbulent flows. The distinction between the two is not always made; however, from unsteady pressure fluctuation measurements of Arakeri (1974) and Huang & Hannan (1975) we might expect the region of flow transition to be far more critically important for cavitation inception than the region of fully developed turbulent flow.

Therefore, for flows with gross separated regions, turbulence effects can dominate in determining the conditions for cavitation inception. It is also under these flow conditions that gaseous cavitation is likely to occur since the nuclei could be subjected to low pressures for significant periods of time, if they are trapped in the core of vortices downstream of flow separation. Based on equilibrium ideas, Holl (1960a) has proposed the scaling law

$$\sigma_i = -C_p + (p_g / \frac{1}{2} \rho U^2), \quad p_g = \alpha \beta, \quad (17)$$

for predicting the value of σ_i due to gaseous cavitation. Here C_p is the pressure coefficient at the expected location of inception, α is the dissolved gas content and β , the Henry's law constant. The observed values of σ_i for hub vortex flows have been predicted with reasonable accuracy using the scaling law (Arndt 1974). Whenever, the danger of gaseous cavitation is likely, then σ_i for this type of cavitation should be compared with the σ_i estimated for vaporous cavitation based on one of the appropriate correlations proposed earlier and the higher value of σ_i should be taken as critical.

4.4 Remarks on viscous effects

From the present considerations we note that certain subtle features of boundary layer flow like laminar separation and the location of turbulent transition have an important effect on cavitation inception. The viscous effects manifest themselves in altering the pressure field as compared to that which would exist under the assumptions of potential flow. In particular, the presence of unsteady pressures is entirely due to viscous effects. We would anticipate from the well-known laws of similarity that the mean static pressure field would scale with the dynamic head, $\frac{1}{2} \rho U^2$, except for flows with the presence of laminar separated regions. The crucial question then is, do the unsteady pressures also scale simply with the dynamic head? If they do not, then we would expect scale effects in cavitation inception which takes place within the boundary layer regions of the flow and where unsteady pressures do exist.

Another important point to note is that besides alteration in the pressure field, viscous effects can play a crucial role in the formation of attached cavities on a body. This results from the fact that the surface of an attached cavity is a boundary of zero shear stress and for its formation a compatible condition of zero shear stress at the wall should exist at some point within the boundary layer flow. This compatible condition is readily satisfied in the presence of laminar separation and for this reason attached cavities are mostly associated with the region of laminar separation. As evident from the results of cavitation inception on a tripped body, attached cavities in the absence of separation are difficult if not impossible to sustain. In view of these

observations, it should be pointed out that the existence of laminar separation is not always limited to low Reynolds number flows and for certain body shapes this feature can persist even upto a Reynolds number of ten million. For example, on a hemispherically nosed body, laminar separation was observed at a Reynolds number of one million and based on calculations, it is expected that it may persist upto a Reynolds number of five million (Arakeri 1973). In addition, the flow downstream of a surface irregularity can have the same properties as flow in the neighbourhood of normally occurring laminar separation (Klebanoff & Tidstrom 1972). Therefore, even if laminar separation is not normally possible due to either the body shape at high body Reynolds numbers, locally the condition of zero shear stress may still be satisfied as a result of the presence of surface irregularities and attached cavities may form at these locations.

5. Thermodynamic effects

When a bubble grows by vaporisation a certain amount of energy is required to convert some quantity of liquid to vapour. The energy supply will result in a local drop in the temperature of the liquid near the bubble surface. If this drop is negligible compared to the bulk liquid temperature then the bubble growth is limited only by dynamic means and the process is known as cavitation. However, if the drop is significant then the bubble growth is limited by a heat transfer process which enables the temperature near the surface to increase. The process where the bubble growth is limited by heat transfer or thermodynamic effect is known as boiling. It is important to distinguish between the two since the bubble growth rates are quite different in the two processes (Holl & Kornhauser 1970). Even though the boundaries for water are fairly well established, the same cannot be said for cryogenic liquids used in rocket propulsion applications, petroleum products used in chemical industry and liquid metals used as coolants for reactor applications.

Brennen (1973) has derived a criterion which enables one to predict *a priori* whether cavitation or boiling will dominate in a given situation. In the present paper, the same criterion is derived with a much simpler formulation but based on Brennen's assumptions. First we look at bubble growth during boiling following the analysis of Plesset (1969). The rate of heat transfer required for vapour formation at the bubble surface of radius R is given by,

$$\dot{Q} = \mathcal{L} \frac{d}{dt} (\frac{4}{3} \pi R^3 \rho_v) \doteq 4\pi R^2 \dot{R} \mathcal{L} \rho_v, \quad (18)$$

where \mathcal{L} is the latent heat of vaporisation, ρ_v is the vapour density and the dot represents the derivative with respect to time. It is assumed here that the term proportional to $d\rho_v/dt$ is negligible in equation (18). This is justified on the basis that the rate of change of bubble temperature is expected to be small. The required heat flow for vaporisation is supplied by the temperature difference between the bubble wall and the bulk of the liquid. The temperature difference will be limited to the diffusion length given by $(D\tau)^{1/2}$ where D is the thermal diffusivity of the liquid and τ is the bubble growth time. If the diffusion length is assumed to be small then the rate of heat flow into the bubble is approximately given by

$$\dot{Q} = 4\pi R^2 k \frac{(T_\infty - T_R)}{(D\tau)^{\frac{1}{2}}}, \quad (19)$$

where k is the coefficient of heat conduction for the liquid, T_∞ is the bulk liquid temperature and T_R is the temperature in the liquid near the bubble surface. Equating the two heat transfer rates we get,

$$\dot{R} = \frac{k(T_\infty - T_R)}{\mathcal{L} \rho_v (D\tau)^{\frac{1}{2}}}. \quad (20)$$

This equation for \dot{R} will be the basis for the criterion to be derived. We note that the time τ can be taken equal to $(L/U)K_2$, L is the typical length scale, U the reference velocity and K_2 is a constant. The most logical choice for K_2 is the ratio $(C_{p \min}/\sigma)$; this follows from the fact that the bubble growth will take place mostly in the vicinity of the minimum pressure area and the lower the value of σ the higher the time the bubble will spend in the favourable pressure region of the flow for its growth. In addition, we relate $(T_\infty - T_R)$ to $\{p_v(T_\infty) - p_v(T_R)\}$ using the Clausius-Clapeyron equation, and the result in non-dimensional form is

$$\frac{p_v(T_R) - p_v(T_\infty)}{\frac{1}{2}\rho U^2} = C_T = \frac{-\mathcal{L} \rho_v (T_R - T_\infty)}{T_\infty \frac{1}{2}\rho U^2}, \quad (21)$$

where p_v is the vapour pressure at the corresponding temperature. Substituting (21) along with the estimate for τ in (20), we get

$$\frac{dr_1}{dt_1} = \frac{C_T T_\infty D^{\frac{1}{2}} c^p \rho^2}{2(-C_{p \min})^{\frac{1}{2}} \mathcal{L}^2 \rho_v^2} (U^3 \sigma / L)^{\frac{1}{2}}, \quad (22)$$

where r_1 is R/L , t_1 is tU/L and c^p is the specific heat of the liquid. Returning to the condition of boiling, that inertial terms are negligible in the dynamic equation for bubble growth (see Holl 1969 or Brennen 1973) and since all other terms, excluding $(-C_p - \sigma + C_T)$, are also negligible except at the initial stages of growth, we get $C_T = C_{p \min}$, as a result of σ being usually small. Finally using the explicit condition for boiling that $(dr_1/dt_1)^2 \ll |C_{p \min}|$ from equation (22), we get

$$\left\{ \frac{c^p \rho^2 D^{\frac{1}{2}} T_\infty}{2 \mathcal{L}^2 \rho_v^2} (U^3 \sigma / L)^{\frac{1}{2}} \right\}^2 |C_{p \min}| \ll |C_{p \min}|, \quad (23)$$

or defining a thermodynamic parameter $\Sigma(T)$ as

$$\Sigma(T) = 2 \mathcal{L}^2 \rho_v^2 / (c^p \rho^2 D^{\frac{1}{2}} T_\infty), \quad (24)$$

the condition for boiling becomes

$$(U^3 \sigma / L) \ll \dot{\Sigma}(T). \quad (25)$$

Similarly, the condition for cavitation then would be

$$(U^3\sigma/L) \gg \Sigma(T). \quad (26)$$

The thermodynamic parameter $\Sigma(T)$ for water, liquid hydrogen, liquid oxygen and liquid sodium as a function of temperature is plotted in figure 13. To get a feel for the use of figure 13 we estimate $(U^3\sigma/L)^{1/2}$ for a turbopump used in a liquid propellant rocket. Typical values (Brennen 1973) for U , L and σ are 100 m/s, 0.5 m and 0.1 respectively, and it follows that $(U^3\sigma/L)^{1/2}$ is of the order of 400 m/s^{3/2}. Thus, from figure 13 we note that liquid oxygen would cavitate rather than boil below about 70°K, liquid hydrogen would virtually always boil and water would cavitate below about 60°C. Since the thermal diffusivity of liquid metals is rather high we should have some reservations about using the criterion for the case of liquid sodium. It may be recalled that the criterion was derived on the basis of assuming a small diffusion length. Due to their high thermal diffusivities it is likely that liquid metals tend to cavitate at even higher temperatures than indicated by the present criterion. Therefore, the prediction of cavitation aspects using the criterion will be conservative. In any case, a rough estimate of $(U^3\sigma/L)^{1/2}$ for a breeder reactor primary pump is 140 m/s^{3/2} (Arakeri & Misra 1974) and we note from figure 13 that liquid sodium will cavitate rather than boil at the operating temperature of 560°C. Therefore, since the present prediction is conservative we can conclude that it should be possible to adequately predict cavitation inception in liquid sodium (at 560°C) based on the existing cavitation inception data for cold water.

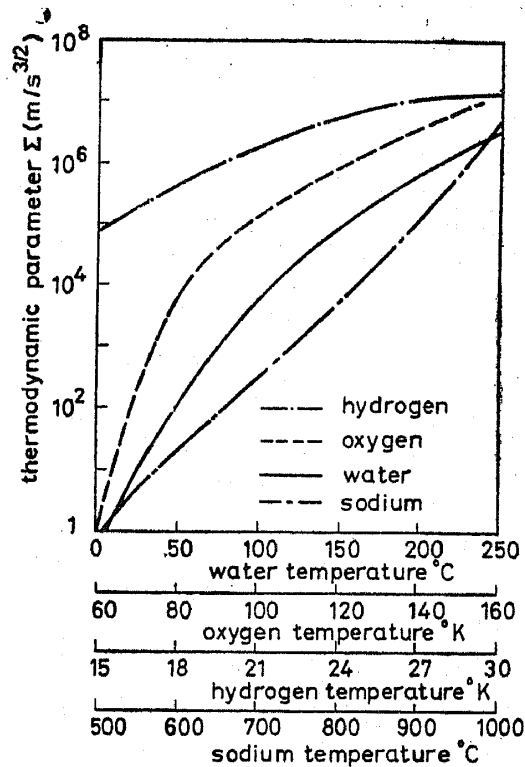


Figure 13. The thermodynamic parameter Σ in m/s^{3/2} for water, oxygen, hydrogen and liquid sodium. (Brennen 1973 and Arakeri & Misra 1974.)

6. Conclusions

We can delineate three different forms of cavitation at inception, the travelling bubble type, the surface or attached type and the vortex type. In a given situation, the type observed will depend on the nuclei content of the liquid and the viscous flow regime. It is important to distinguish between the three types because each is subject to different scaling laws. As may be expected, it is found that the vortex type of cavitation inception is strongly influenced by viscous effects, and σ_i is found to be primarily a function of Reynolds number for this type of cavitation. However, a somewhat unexpected finding is that the surface or attached type of cavitation inception commonly observed on smooth body shapes is also influenced by viscous effects. With the development of improved flow visualisation techniques in water at high Reynolds numbers, it has been found that this type of cavitation is closely connected with the region of laminar separation, if present, and with the location of turbulent transition in the absence of separation. In addition, any modification of the basic viscous flow due to the presence of disturbances is found to have a strong influence on cavitation inception. Scaling laws are suggested to predict σ_i for different viscous flow regimes, namely, flows with laminar separation, turbulent transition without separation, surface roughness and turbulence. Besides viscous effects, cavitation inception is also influenced by the nuclei content of the liquid, gaseous diffusion and thermodynamic effects. To minimise thermodynamic effects and scale effects due to gaseous diffusion, we should ascertain that if these effects are important in prototype situations, then they would also be important under the conditions of model-testing. The possible scale effects due to nuclei content is a difficult question since very little information is available concerning the nuclei content of the liquid to be encountered in various prototype situations.

Even though we now have a better understanding of the physical processes involved in cavitation inception, theoretical prediction of σ_i still appears to be a difficult task. The major stumbling block in further progress will be the lack of knowledge about pressure fields within transitional and turbulent flows. Therefore, in most cases, estimations of σ_i will still have to be based on existing empirical correlations or on model-testing with improved methods of data interpretation.

List of symbols

C	constant in equation (10) and figure 12
C_f	coefficient of friction in turbulent flows
C_p	pressure coefficient, $(p-p_\infty)/\frac{1}{2}\rho U^2$
$C_{p \min}$	minimum pressure coefficient based on P_{\min}
$\overline{C}_{p \min}$	minimum pressure coefficient based on \overline{P}_{\min}
C_{ps}	pressure coefficient at laminar separation
C_{ptr}	pressure coefficient at turbulent transition
C_p'	pressure coefficient based on fluctuating pressures
C_T	thermodynamic coefficient $(p_v(T_R)-p_v(T_\infty))/\frac{1}{2}\rho U^2$
c^p	specific heat of liquid

D	thermal diffusivity of liquid
h	height of isolated surface irregularity
k	heat conductivity of liquid
K_1	constant in equation (13)
K_2	constant to determine τ in equation (20)
L	reference length
\mathcal{L}	latent heat of vaporisation
m, n	constants in equation (10) and figure 12
p	static pressure
$p(R)$	pressure in the liquid at the bubble surface
p_c	critical pressure given by equation (6)
p_g	partial pressure of gas in the bubble
p_{\min}	minimum static pressure
\bar{p}_{\min}	average minimum static pressure in turbulent flows
p_v	vapour pressure of the liquid
p_∞	reference static pressure
p'	unsteady pressure in transitional or turbulent flows
$\overline{p'^2}$	root mean square value of the unsteady pressure
\dot{Q}	heat transfer rate
r_1	non-dimensional bubble radius
R	bubble radius at any time
R_0	initial bubble radius
Re	Reynolds number, UD/ν
s	coefficient of surface tension
T_R	temperature in the liquid at the bubble surface
T_∞	bulk temperature of the liquid
t	dimensional time
t_1	non-dimensional time
U	reference velocity
U_e	velocity at the edge of the boundary layer
U_0	mean velocity
u'_1	longitudinal component of turbulence
u'_2	lateral component of turbulence
$\overline{u'_1 u'_2}$	proportional to Reynolds stress in turbulent flows
a	dissolved gas content
β	constant in Henry's law
δ	boundary layer thickness
ν	kinematic viscosity of the liquid
ρ	density of liquid
ρ_v	density of vapour
σ	cavitation number, $(p_\infty - p_v(T_\infty))/\frac{1}{2} \rho U^2$

- σ_i incipient cavitation number
- $\sigma_{i,f}$ incipient cavitation number for distributed or isolated roughness on a flat plate
- $\sigma_{i,R}$ incipient cavitation number for distributed or isolated roughness on an arbitrary body
- Σ thermodynamic parameter given by equation (24)
- τ time for bubble growth
- τ_0 skin friction in turbulent flow

References

- Arakeri V H 1973 *Viscous effects in inception and development of cavitation on axisymmetric bodies* Ph.D. Thesis, California Institute of Technology
- Arakeri V H 1974 *J. Fluids Eng.* **97** 82
- Arakeri V H and Acosta A J 1973 *J. Fluids Eng.* **95** 519
- Arakeri V H & Acosta A J 1974 *Proc. Seventh Am. Towing Tank Conf., Pasadena*, eds T Y Wu and J W Hoyt (Pasadena: Caltech) p. 233
- Arakeri V H & Acosta A J 1976 *J. Ship Res.* **20** 40
- Arakeri V H & Misra B 1974 Study of potential cavitation in LMFBR components, Tech. Memo. No. ANL-CT. 74-03, Argonne National Laboratory
- Arndt R E A 1974 *Trans. Seventh Int. Assn. for Hydraulic Res. Symp., Vienna (Austria)*
- Arndt R E A & Ippen A T 1968 *J. Basic Eng.* **90** 249
- Blake W K 1970 *J. Fluid Mech.* **44** 637
- Bohn J C 1972 *The influence of surface irregularities on cavitation*. M.Sc. Thesis, Pennsylvania State University
- Brennen C 1973 *J. Fluids Eng.* **95** 533
- Curle N & Skan S W 1957 *Aeronaut. Q.* **8** 257
- Epsten P S & Plesset M S 1950 *J. Chem. Phys.* **18** 1505
- Ellis A T, Waugh J G & Ting R Y 1970 *J. Basic Eng.* **92** 405
- Flynn H G 1964 *Physical acoustics* ed. W P Mason (New York: Academic Press) **1** (part B) p. 127
- Fuchs H V 1972 *J. Sound Vib.* **23** 217
- Gates E M 1977 *The influence of freestream turbulence, freestream nuclei population and a drag reducing polymer on cavitation inception on two axisymmetric bodies*, Ph.D. Thesis, California Institute of Technology
- Harvey E N, McElroy W D & Whiteley A H 1974 *J. Appl. Phys.* **18** 162
- Holl J W 1960a *J. Basic Eng.* **82** 169
- Holl J W 1960b *J. Basic Eng.* **82** 941
- Holl J W 1969 *Cavitation state of knowledge* (New York: ASME) p. 26
- Holl J W & Kornhauser A L 1970 *J. Basic Eng.* **92** 44
- Holl J W & Wislicenus G E 1961 *J. Basic Eng.* **83** 385
- Huang T T & Hannan D E 1975 Pressure fluctuations in the regions of flow transition. Rep. No. 4723, Naval Ship Res. & Dev. Centre, Washington, DC
- Huang T T & Peterson F B 1976 *J. Ship Res.* **20** 215
- Jaffe N A, Okamura T T and Smith A M O 1970 *AIAA J.* **8** 301
- Johnson V E & Hsieh T 1966 *Sixth symposium in naval hydrodynamics, Washington*, Office of Naval Res., US Dept. of Navy
- Johnson C A 1969 *Proc. Twelfth Int. Towing Tank Conf., Rome*, p. 381
- Keller A P 1972 *J. Basic Eng.* **94** 917
- Keller A P 1974 Conference on Cavitation, paper No. C 159/74, Edinburgh (Scotland) p. 109
- Kermeen R W & Parkin B R 1957 Incipient cavitation and wake flow behind sharp edged disks, Rep. No. Engg. 85-4, California Institute of Technology
- Klebanoff R S & Tidstrom K D 1972 *Phys. Fluids* **15** 1173

- Knapp R T, Daily J W & Hammitt F G 1970 *Cavitation* (New York: McGraw Hill) Ch. 1
- Knapp R T & Hollander A 1948 *Trans. ASME* 70 419
- Lindgren H & Johnson C A 1966 *Proc. Eleventh Int. Towing Tank Conf., Tokyo*
- Morgan W B 1972 *Proc. Thirteenth Int. Towing Tank Conf., Berlin*
- Oosterveld M W C 1977 Private communication
- Oshima R 1961 *J. Basic Eng.* 83 379
- Parkin B R 1952 *Scale effects in cavitating flow*, Ph.D. Thesis, California Institute of Technology
- Parkin B R & Holl J W 1954 Incipient cavitation scaling experiments for hemispherical and 1.5 caliber ogive-nosed bodies. Rep. Nord. 7958-264, Pennsylvania State University
- Parkin B R & Kermeen R W 1953 Incipient cavitation and boundary layer interaction on streamlined body. Rep. No. Engg. 35.2, California Institute of Technology
- Peterson F B 1972 *Ninth symposium on naval hydrodynamics, Washington*, Office of Naval Res., US Dept. of Navy
- Plesset M S 1949 *J. Appl. Mech.* 16 277
- Plesset M S 1969 Cavitating flows, Rep. No. Engg. 85-146, California Institute of Technology
- Ripken J F & Killen J M 1962 *Proc. Int. Assn. for Hydraulic Res. Symp., Sendai (Japan)*
- Shiebe F R 1969 The influence of gas nuclei size distribution on transient cavitation near inception St. Anthony Falls Hydraulics Lab. Rep. No. 107, University of Minnesota
- Tani I 1961 *Boundary layer and flow control* ed. G. Lachmann (New York: Pergamon) 2 637
- Van der Muelen J H J 1976 *A holographic study of cavitation on axisymmetric bodies and the influence of polymer additives*, Ph.D. Thesis, University of Enschede, Holland
- Van der Walle F 1962 *Fourth Symp. on naval hydrodynamics, Washington*, Office of Naval Res., US Dept. of Navy
- Van Driest E R and Blummer C B 1968 *AIAA J.* 1 1303



Plate 1

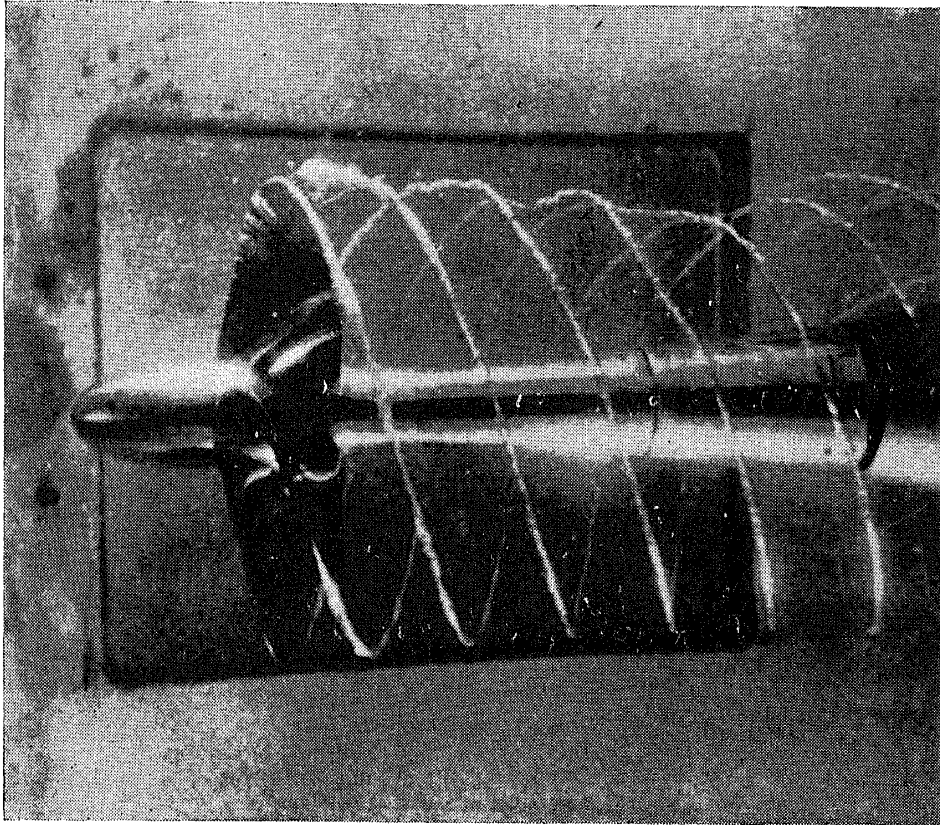


Figure 1. Tip vortex cavitation on a model ship propeller. (Photograph courtesy of Netherlands Ship Model Basin)

Plate 2

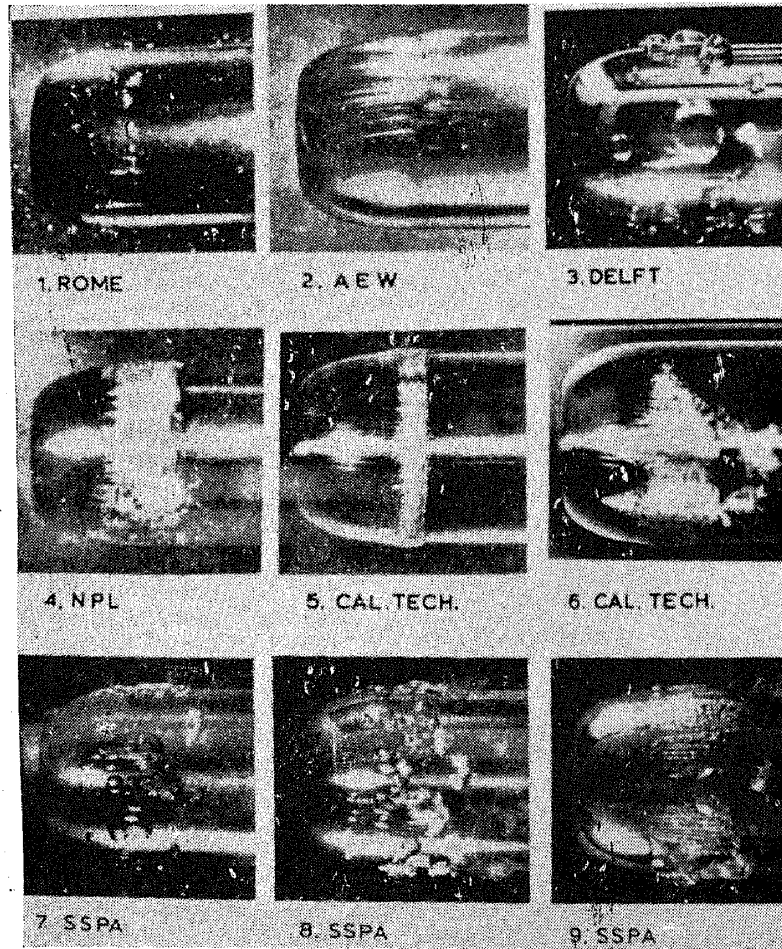


Figure 7. Nature and form of cavitation at inception observed on geometrically similar axisymmetric headforms with modified ellipsoidal nose in various tunnel facilities (Johnson 1969).

Plate 3

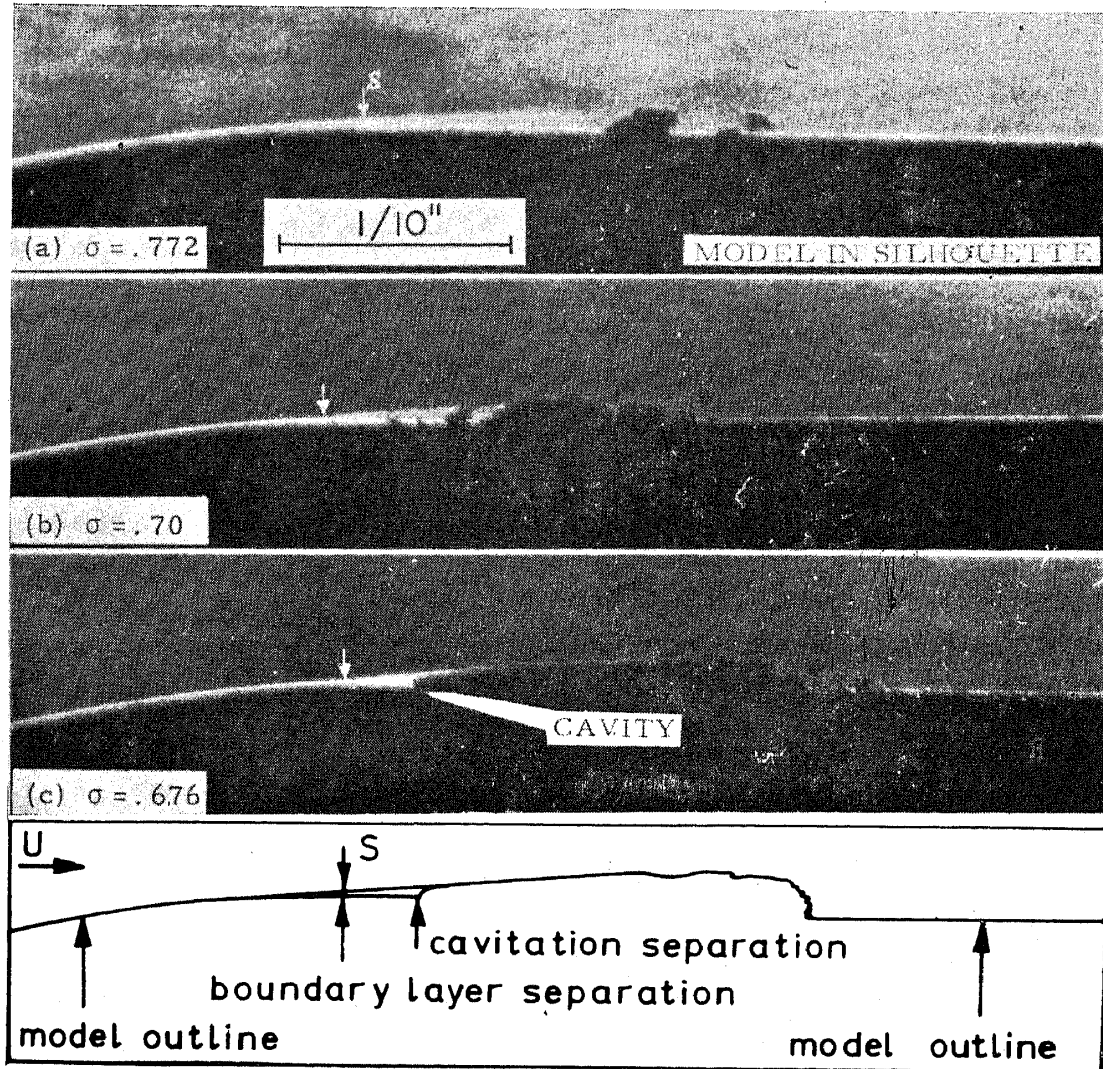


Figure 10. Cavitation inception on a hemispherically-nosed body as influenced by the presence of laminar boundary layer separation. The white arrow marks the location of separation observed by the Schlieren technique. The dark patches above model outline are cavitating areas. The flow is from left to right (Arakeri & Acosta 1973).